

Analysis of Transients in a Three-Level DC–DC Flying Capacitor Converter: Time Domain Approach

Research Article

Boris Reznikov¹, Dr. Alexander Ruderman², Dr. Valentina Galanina³

¹ Engineering Company Satprof LLC, Gelsingforsskaya Str., 4, Build. 1, Lit. B, St. Petersburg, 194044, Russian Federation, Russia

² Nazarbayev University, Kabanbay Batyr Ave., 53, Nur-Sultan 010000, Kazakhstan, Israel

³ State University of Aerospace Instrumentation, Bolshaya Morskaya Str. 67, Lit. A, St. Petersburg, 190000, Russian Federation, Russia

Received December 23, 2018; Accepted March 13, 2019

Abstract: The paper considers a discrete state-space model for transients in a three-level flying capacitor DC–DC converter. A transition matrix is obtained for a pulse width modulation (PWM) period. The matrix elements are expanded into a power series using a selected small parameter. The matrix eigenvalues that determine the natural balancing dynamics transients are presented in the form of power series as well. Four separate transients are constructed based on four possible PWM period initial states (topologies). Inductor current and capacitor voltage transients are found for the voltage source power-up as the arithmetic average of the four separate transients. The discrete solutions are replaced by continuous ones. The resulting transients that are elementary functions of the circuit parameters, PWM period, and voltage reference demonstrate good agreement with the simulation results.

Keywords: Three-level DC–DC converter • Flying capacitor • Transient • Natural balancing

1. Introduction

Multilevel Flying Capacitor Converter (FCC) was first proposed in 1992 (Meynard and Foch, 1992). The idea of using pulse width modulation (PWM) control of capacitor circuits with natural balancing of voltage for capacitors charged to fractions of the input source voltage seems to be promising, especially, accounting for the technology progress in capacitor fabrication.

Additional reactive elements (capacitors) of a converter circuit certainly slow down its dynamic response. Therefore, it is important to evaluate FCC dynamics, that is, the speed and type of transients in the converter circuit due to an input source power-up or fluctuation (like step-up or step-down variation).

Until recently, FCC natural balancing dynamics transient analysis was dominated by the frequency domain approach (McGrath and Holmes, 2008; Meynard et al., 1997; Wilkinson et al., 2006) that employs infinite Fourier series with Bessel function coefficients. A significant drawback of this approach is the need to take into account the large number of the series terms (30 or more) to obtain good accuracy. Due to the cumbersome form of the series coefficients, it does not reveal dependences on the circuit and load parameters.

An alternative to the frequency domain approach is time domain analysis. Such an analysis was first applied to describe an elementary three-level FCC with a single flying capacitor in 2008 (Margaliot et al., 2011; Ruderman et al., 2008). This was followed by calculations for multi-level FCC up to seven-level (Ruderman and Reznikov, 2011). All these articles provide natural balancing dynamics time constant (and oscillating frequency where applicable) expressions, but the calculation methodology is described very briefly (by literally several phrases) due to the conference paper size limitations. The only exception in this meaning is the paper (Margaliot et al., 2011).

* Email: b_reznikov@mail.ru, alexander.ruderman@nu.edu.kz, va_gal@rambler.ru

Such a scanty theoretical description gives rise to a lot of questions and leads to an incomplete understanding of the proposed analysis essence. In this article, a more general approach to the analysis of a three-level FCC dynamic operation will be presented, as well as more detailed discussion of issues that did not get a necessary explanation in the study by Margaliot et al. (2011).

The purpose of this paper is to obtain simple and accurate formulae that give the dependences of the transient characteristics on the converter circuit and PWM parameters. Such formulae would allow a designer to choose the parameters to meet the transients' performance requirements.

2. The problem formulation. Discrete model

Figure 1a shows a three-level FCC circuit. This is a DC-DC converter with output voltage range being from $-V/2$ to $V/2$, V – DC source voltage.

It is common to make the following assumptions for the FCC analysis. First, the load is represented as a series connection of an inductor and a resistor (RL-load). Second, the switches are supposed ideal meaning, allowing bidirectional conduction with zero resistance in the open state and infinite resistance in the closed one. Switching times are supposed zero.

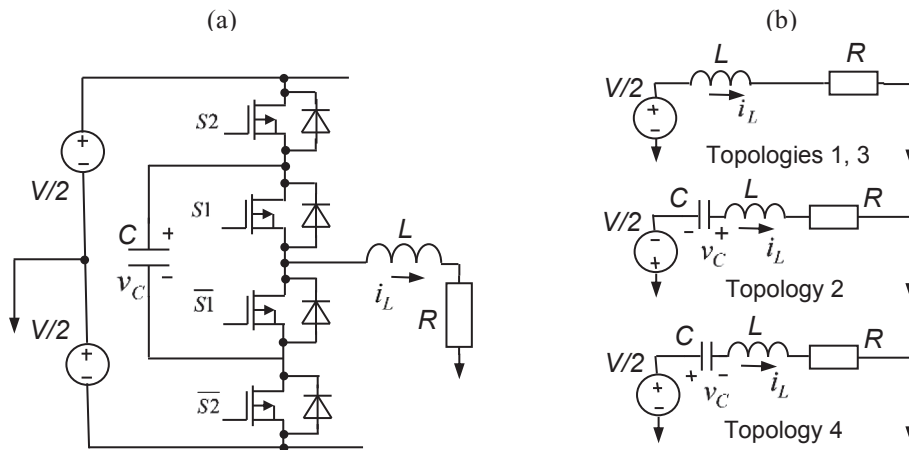


Fig. 1. Electric circuit of a three-level Flying Capacitor Converter (a) and its switched topologies (b)

The modulation strategy (the switching sequences of complementary switch pairs $S1, \overline{S1}$ и $S2, \overline{S2}$ along with the switching state time durations) is considered in detail in the studies by Margaliot et al. (2011) and Ruderman et al. (2008). PWM period T_{PWM} is divided into four successive time intervals $\Delta t_1, \Delta t_2, \Delta t_3, \Delta t_4$. For each interval, there is its own equivalent circuit (topology) of the converter. The duration of the intervals in pairs match, namely, $\Delta t_1 = \Delta t_3$ and $\Delta t_2 = \Delta t_4$.

Figure 1b presents the topologies of the 1st, 2nd, and 4th intervals. The topology of the 3rd interval is identical to that of the 1st one. Switches $S1$ and $S2$ in the ON state define the 1st and 3rd topologies. Switch $S1$ in the ON state and switch $S2$ in the OFF state define the 2nd topology, and, finally, switch $S2$ in the ON state and $S1$ in the OFF state define the 4th topology.

As shown in the study by Ruderman et al. (2008), the durations of the 1st and 2nd intervals are related to the reference voltage (normalised voltage command) $D, -1 < D < 1$, by the ratios

$$\Delta t_1 = \frac{|D|}{2} T_{\text{PWM}} \quad (1)$$

$$\Delta t_2 = \frac{1 - |D|}{2} T_{\text{PWM}} \quad (2)$$

Due to the symmetry, considered are only positive values of D , $0 < D < 1$.

From Figure 1b, it is seen that the topologies of each interval are the 1st or 2nd-order linear circuits. Therefore, if the inductor current i_L and capacitor voltage v_C are known at the moment t – the beginning of time interval k – their values at the end of the interval, that is, at the moment $t + \Delta t_k$, can be calculated analytically by solving the corresponding differential equations. Let $X(t) = (i_L(t) \ v_C(t))^T$ be a state-space vector. Then for time interval Δt_k

$$X(t + \Delta t_k) = A_k(\Delta t_k)X(t) + B_k(\Delta t_k)\frac{V}{2}, \quad (3)$$

where matrices A_k and vectors B_k are as follows:

$$A_1(\tau) = A_3(\tau) = \begin{pmatrix} \exp(-2\alpha\tau) & 0 \\ 0 & 1 \end{pmatrix}; \quad (4)$$

$$A_2(\tau) = \exp(-\alpha\tau) \begin{pmatrix} \cos\omega\tau - \frac{\alpha}{\omega}\sin\omega\tau & \frac{1}{\omega L}\sin\omega\tau \\ -\frac{1}{\omega C}\sin\omega\tau & \cos\omega\tau + \frac{\alpha}{\omega}\sin\omega\tau \end{pmatrix}; \quad (5)$$

$$A_4(\tau) = \exp(-\alpha\tau) \begin{pmatrix} \cos\omega\tau - \frac{\alpha}{\omega}\sin\omega\tau & -\frac{1}{\omega L}\sin\omega\tau \\ \frac{1}{\omega C}\sin\omega\tau & \cos\omega\tau + \frac{\alpha}{\omega}\sin\omega\tau \end{pmatrix}; \quad (6)$$

$$B_1(\tau) = B_3(\tau) = \begin{pmatrix} \frac{1 - \exp(-2\alpha\tau)}{R} \\ 0 \end{pmatrix}; \quad (7)$$

$$B_2(\tau) = \begin{pmatrix} -\exp(-\alpha\tau)\frac{\sin\omega\tau}{\omega L} \\ 1 - \exp(-\alpha\tau)\left(\cos\omega\tau + \frac{\alpha}{\omega}\sin\omega\tau\right) \end{pmatrix}; \quad (8)$$

$$B_4(\tau) = \begin{pmatrix} \exp(-\alpha\tau)\frac{\sin\omega\tau}{\omega L} \\ 1 - \exp(-\alpha\tau)\left(\cos\omega\tau + \frac{\alpha}{\omega}\sin\omega\tau\right) \end{pmatrix}, \quad (9)$$

$$\alpha = \frac{R}{2L}, \omega = \sqrt{\omega_0^2 - \alpha^2}, \omega_0^2 = \frac{1}{LC}.$$

Due to the inductor current and capacitor voltage continuity at the switching moments, their final values at the end of an interval Δt_k can be considered as initial values for a consecutive one. Thus, using equation (3) for each of the four intervals of the PWM period, it is possible to obtain a relationship between the state-space vectors at the beginning and at the end of the PWM period, starting from the 1st interval and ending with the 4th. Let the sequence

of intervals 1–2–3–4 have the number 1. This number will be displayed as a superscript in parentheses. The other three possible sequences will be considered below. Thus,

$$X^{(1)}(t + T_{\text{PWM}}) = A^{(1)}X(t) + B^{(1)}\frac{V}{2}, \quad (10)$$

where transient matrix $A^{(1)}$ and vector $B^{(1)}$ are found as follows:

$$A^{(1)} = A_4(\Delta t_4)A_3(\Delta t_3)A_2(\Delta t_2)A_1(\Delta t_1) \quad (11)$$

$$B^{(1)} = A_4(\Delta t_4)\left(A_3(\Delta t_3)\left(A_2(\Delta t_2)B_1(\Delta t_1) + B_2(\Delta t_2)\right) + B_3(\Delta t_3)\right) + B_4(\Delta t_4). \quad (12)$$

Matrix $A^{(1)}$ and vector $B^{(1)}$ completely determine the behaviour of the converter at discrete time instants nT_{PWM} , $n = 1, 2, 3, \dots$. The use of equation (10) means the transition to a discrete system, which causes a loss of information about FCC behaviour between discrete time samples, that is, within a PWM period. In other words, equation (10) describes the process of changing the state of a circuit in a “long” time and ignores fast oscillations in a “short” time, caused by the switching within a PWM period. These fast oscillations present a noise or ripple superimposed on a slow dynamic process in a “long” time and determine a quality of the load current and the capacitor voltage. This paper does not consider fast processes and focuses only on slow dynamic processes.

Let us rewrite equation (10) as:

$$X^{(1)}(t_{k+1}) = A^{(1)}X(t_k) + B^{(1)}\frac{V}{2}, \quad t_{k+1} = t_k + T_{\text{PWM}}. \quad (13)$$

The FCC transient behaviour described by the system of difference equation (13) depends on matrix $A^{(1)}$ eigenvalues. Starting the PWM period from the 2nd, 3rd, or 4th interval will result in three other matrices $A^{(n)}$ and vectors $B^{(n)}$ due to cyclic permutation of matrix factors in equation (11) and cyclic indices shift in equation (12).

Each of the four matrices $A^{(n)}$ corresponds to its own transition process, which will be referred to as a partial transient. Note that all these matrices have the same eigenvalues, meaning the same behaviour of partial transients.

In the study by Ruderman et al. (2008), matrix $A^{(1)}$ is calculated exactly in accordance with equation (11). Even for an elementary single capacitor three-level FCC, the matrix elements are rather cumbersome. For a FCC with a larger number of levels (capacitors), accurate calculation of the matrix elements becomes problematic and finding the exact eigenvalues – “mission impossible”.

As it often happens in similar situations, a suitable small parameter may come to the rescue. In our specific case, modulation period subinterval time durations are sufficiently small so that the load current and capacitor voltage do not have enough time to significantly deviate from their linear trend. In particular, this means that for any reference D , the arguments of functions $\sin\omega\tau$, $\cos\omega\tau$, $\exp(-\alpha\tau)$ are small. From equations (1) and (2), the maximum switching interval duration is $\Delta t_i = T_{\text{PWM}}/2$, which means that the parameter $\delta = \omega T_{\text{PWM}}/2$ is small. But if δ is small, then the parameter $\beta = 2\delta = \omega T_{\text{PWM}}$ is small to the same extent. So, in the rest of the paper, β will be used as the small parameter.

Let us rewrite matrices $A_k(\Delta t_k)$ expressions in such a way that their elements are functions of β . For that first denote $r = \frac{\alpha}{\omega}$, $\beta_1 = \beta(1 - D)/2$ and also note that $\alpha\Delta t_1 = \alpha\Delta t_3 = \beta r D/2$ and $\alpha\Delta t_2 = \alpha\Delta t_4 = r\beta_1$. Then,

$$A_1(\Delta t_1) = A_3(\Delta t_3) = \begin{pmatrix} \exp(-rD\beta) & 0 \\ 0 & 1 \end{pmatrix}; \quad (14)$$

$$A_2(\Delta t_2) = \exp(-r\beta_1) \begin{pmatrix} \cos\beta_1 - r \cdot \sin\beta_1 & \frac{1}{\omega L} \sin\beta_1 \\ -\omega L(1+r^2)\sin\beta_1 & \cos\beta_1 + r \cdot \sin\beta_1 \end{pmatrix}; \quad (15)$$

$$A_4(\Delta t_4) = \exp(-r\beta_1) \begin{pmatrix} \cos\beta_1 - r \cdot \sin\beta_1 & -\frac{1}{\omega L} \sin\beta_1 \\ \omega L(1+r^2)\sin\beta_1 & \cos\beta_1 + r \cdot \sin\beta_1 \end{pmatrix}. \quad (16)$$

3. Eigenvalues

Let us present the elements of matrices A_i as power series of β and find a matrix product according to equation (11) to have the elements of the transient matrix $A^{(1)}$ in the form of power series as well. The result will be:

$$A^{(1)} = \begin{pmatrix} a_{11} & a_{12} \\ a_{21} & a_{22} \end{pmatrix}, \quad (17)$$

where

$$a_{11} = 1 - 2r\beta + 2r^2\beta^2 + \frac{r}{12} \left((1+r^2)(D^3 - 3D) + 2 - 14r^2 \right) \beta^3 + \dots; \quad (18)$$

$$a_{12} = \frac{r}{2} \frac{D-1}{\omega L} \beta^2 + \frac{r^2}{4} \frac{(D-1)^2 (D-2)}{\omega L} \beta^3 + \dots; \quad (19)$$

$$a_{21} = \omega L r (1+r^2) (D-1) \beta^2 + \frac{r^2}{4} \omega L (1+r^2) (D-1) (D+2) \beta^3 + \dots; \quad (20)$$

$$a_{22} = 1 - \frac{r}{12} (1+r^2) (D-1)^2 (D+2) \beta^3 + \dots \quad (21)$$

Matrix $A^{(1)}$ eigenvalues are the roots of the characteristic polynomial $p(\lambda) = \det(A^{(1)} - \lambda E)$, where E – 2×2 unity matrix. The polynomial coefficients found using the matrix elements (18)–(21) can be presented in the form of power series expansion

$$p(\lambda) = \lambda^2 + g_1 \lambda + g_2, \quad (22)$$

$$g_1 = -2 + 2r\beta - 2r^2\beta^2 + \frac{4}{3} r^3 \beta^3 + \frac{r^2}{12} \left((1+r^2)(2D^3 - 3D^2) + 1 - 7r^2 \right) \beta^4 + \dots;$$

$$g_2 = -1 + 2r\beta + 2r^2\beta^2 - \frac{4}{3} r^3 \beta^3 + \frac{2}{3} r^4 \beta^4 + \dots$$

The polynomial roots can be found by solving the quadratic equation (22) as shown in the study by Ruderman et al. (2008). However, this paper suggests a more general approach to finding the roots that are sought in the form of a power series expansion. The suggested approach is universal and does not depend on the order of the polynomial. So, the roots of equation (22) are sought in the form

$$\lambda_i = u_0^{(i)} + u_1^{(i)} \beta + u_2^{(i)} \beta^2 + u_3^{(i)} \beta^3 + \dots, \quad i = 1, 2. \quad (23)$$

Since the polynomial coefficients are represented by the converging series and the roots are expressed as explicit functions of the coefficients using additions and multiplications and raised to the power of $1/2$, the series representing the roots will also converge. After substitution of equation (23) into (22) and equating to zero, the characteristic equation in the form of power series expansion becomes

$$p(\lambda_i) = c_0^{(i)} + c_1^{(i)} \beta + c_2^{(i)} \beta^2 + c_3^{(i)} \beta^3 + c_4^{(i)} \beta^4 + \dots = 0, \quad (24)$$

where

$$\begin{aligned}
c_0^{(i)} &= (u_0^{(i)} - 1)^2; c_1^{(i)} = 2(u_0^{(i)} - 1)(r + u_1^{(i)}); \\
c_2^{(i)} &= 2(u_0^{(i)} - 1)(u_2^{(i)} - r^2) + u_1^{(i)}(2r + u_1^{(i)}); \\
c_3^{(i)} &= (u_0^{(i)} - 1)\left(2u_3^{(i)} + \frac{4}{3}r^3\right) + 2(ru_2^{(i)} - r^2u_1^{(i)} + u_1^{(i)}u_2^{(i)}); \\
c_4^{(i)} &= u_0^{(i)}\frac{r^2}{12}f(D) + \frac{2}{3}r^3(r + 2u_1^{(i)}) + 2(ru_3^{(i)} - r^2u_2^{(i)} + u_1^{(i)}u_2^{(i)}); \\
f(D) &= (1 + r^2)(2D^3 - 3D^2 - 7) + 8.
\end{aligned}$$

To ensure $p(\lambda_i) = 0$, the necessary and sufficient condition is to have all the coefficients $c_k^{(i)}$ equal to zero. Sequential finding of coefficients $u_j^{(i)}$, starting with lower power, leads to $u_0^{(1)} = 1$, $u_1^{(1)} = -2r$, $u_2^{(1)} = 2r^2$, $u_3^{(1)} = \frac{r}{24}((1+r^2)(2D^3 - 3D^2 + 1) - 32r^2)$ for the first root and $u_0^{(2)} = 1$, $u_1^{(2)} = 0$, $u_2^{(2)} = 0$, $u_3^{(2)} = -\frac{r}{24}(1+r^2)(2D^3 - 3D^2 + 1)$ for the second one. This way, the roots of equation (24) are expressed as

$$\lambda_1 = 1 - 2r\beta + 2r^2\beta^2 + \frac{r}{24}((1+r^2)(2D^3 - 3D^2 + 1) - 32r^2)\beta^3 + O(\beta^4). \quad (25)$$

$$\lambda_2 = 1 - \frac{r}{24}(1+r^2)(2D^3 - 3D^2 + 1)\beta^3 + O(\beta^4). \quad (26)$$

Based on equations (25) and (26), it is possible to make a formal conclusion about the discrete system stability because both the roots are less than unity, which means the general solution strives to zero when time strives to infinity.

4. Particular solution of the homogeneous system

Let us find a general solution of the system of difference equations (13) written in matrix form. As the eigenvalues λ_1 and λ_2 are different, there are two different corresponding eigenfunctions λ_1^k and λ_2^k , where the integer k refers to the number of discrete time sample. The system has two eigenvectors – $\Gamma_1 = \lambda_1^k \begin{pmatrix} \gamma_1^{(1)} & \gamma_2^{(1)} \end{pmatrix}$ and $\Gamma_2 = \lambda_2^k \begin{pmatrix} \gamma_1^{(2)} & \gamma_2^{(2)} \end{pmatrix}$ – corresponding to each eigenvalue in equations (25) and (26). An eigenvector is determined up to the constant factor. Therefore, one of its components may be selected arbitrary. Let us choose $\gamma_1^{(1)} = 1$ and $\gamma_1^{(2)} = 1$. Then, the second eigenvector coordinates are found from the set of linear equations

$$\begin{pmatrix} a_{11} - \lambda_i & a_{12} \\ a_{21} & a_{22} - \lambda_i \end{pmatrix} \begin{pmatrix} 1 \\ \gamma_2^{(i)} \end{pmatrix} = 0. \quad (27)$$

As equation (27) is linearly dependent, either of them can be used for $\gamma_2^{(i)}$ determination. By alternately substituting λ_1 and λ_2 in equation (27) and making a power series expansion, the eigenvectors components may be obtained as

$$\gamma_2^{(1)} = \frac{\omega L}{4}(1+r^2)(1-D)\beta - \frac{\omega L}{8}(1+r^2)(1-D)rD\beta^2 + O(\beta^3); \quad (28)$$

$$\gamma_2^{(2)} = -\frac{4\omega L}{1-D}\beta^{-1} + \frac{2\omega LrD}{1-D}\beta^0 + O(\beta^1). \quad (29)$$

The general solution of equation (13) can be written as:

$$X^{(1)}(k) = Q_1 \lambda_1^k \begin{pmatrix} 1 \\ \gamma_2^{(1)} \end{pmatrix} + Q_2 \lambda_2^k \begin{pmatrix} 1 \\ \gamma_2^{(2)} \end{pmatrix}, \quad (30)$$

where Q_1 and Q_2 are arbitrary constants.

Using the general solution, let us find a particular solution of a homogeneous system, that is, the solution for zero source voltage. Suppose that at the initial moment for $k=0$ the inductor current equals $i_L(0)$ and the capacitor voltage – $v_C(0)$, then equation (30) can be rewritten as:

$$\begin{pmatrix} i_L(0) \\ v_C(0) \end{pmatrix} = Q_1 \begin{pmatrix} 1 \\ \gamma_2^{(1)} \end{pmatrix} + Q_2 \begin{pmatrix} 1 \\ \gamma_2^{(2)} \end{pmatrix}. \quad (31)$$

The solution of equation (31) with respect to Q_1 and Q_2 becomes

$$Q_1 = \frac{\gamma_2^{(2)}}{\gamma_2^{(2)} - \gamma_2^{(1)}} i_L(0) - \frac{1}{\gamma_2^{(2)} - \gamma_2^{(1)}} v_C(0); \quad (32)$$

$$Q_2 = -\frac{\gamma_2^{(1)}}{\gamma_2^{(2)} - \gamma_2^{(1)}} i_L(0) + \frac{1}{\gamma_2^{(2)} - \gamma_2^{(1)}} v_C(0). \quad (33)$$

After substituting the expressions for $\gamma_2^{(1)}$ and $\gamma_2^{(2)}$ from equations (28) and (29) into (32) and (33) and series expansion of $i_L(0)$ and $v_C(0)$ coefficients, the solution for Q_1 and Q_2 is found to be:

$$Q_1 = \left(1 + O(\beta^2)\right) i_L(0) + \left(\frac{1-D}{4\omega L} \beta + \frac{1-D}{8\omega L} rD\beta^2 + O(\beta^3)\right) v_C(0); \quad (34)$$

$$Q_2 = \left(\frac{1+r^2}{16} (1-D)^2 \beta^2 + O(\beta^4)\right) i_L(0) - \left(\frac{1-D}{4\omega L} \beta + \frac{1-D}{8\omega L} rD\beta^2 + O(\beta^3)\right) v_C(0). \quad (35)$$

This way, by substitution of equations (34) and (35) into equation (31), the particular solution of the homogeneous system becomes:

$$i_L(k) = F_{11} \lambda_1^k + F_{12} \lambda_2^k; \quad (36)$$

$$v_C(k) = F_{21} \lambda_1^k + F_{22} \lambda_2^k, \quad (37)$$

$$F_{11} = \left(1 + O(\beta^2)\right) i_L(0) + \left(\frac{1-D}{4\omega L} \beta + O(\beta^2)\right) v_C(0); \quad (38)$$

$$F_{12} = \left(\frac{1+r^2}{16} (1-D)^2 \beta^2 + O(\beta^4)\right) i_L(0) - \left(\frac{1-D}{4\omega L} \beta + O(\beta^2)\right) v_C(0); \quad (39)$$

$$F_{21} = \left(\frac{\omega L(1+r^2)}{4} (1-D) \beta + O(\beta^2)\right) i_L(0) + \left(\frac{(1+r^2)}{16} (1-D)^2 \beta^2 + O(\beta^4)\right) v_C(0); \quad (40)$$

$$F_{22} = \left(-\frac{\omega L(1+r^2)}{4}(1-D)\beta + O(\beta^2) \right) i_L(0) + \left(1 + O(\beta^2) \right) v_C(0). \quad (41)$$

Note that the series in equations (38)–(41) are represented only by the terms with a minimum power of β . As shown below, even this approximation is sufficient for obtaining an accurate practical result. If it is required to obtain more accurate estimates, the terms with higher powers have to be retained.

5. Partial transients of natural balancing dynamics

To obtain a particular solution for a non-homogeneous system of equations (partial transient), that is, for the case of a non-zero source voltage, one must first find the steady-state values of the inductor current and capacitor voltage (which exists based on the above-noted fact of the system stability).

To do this, first it is necessary to find vector $B^{(1)}$ by equation (12). Similar to the transition matrix $A^{(1)}$ calculation, substitute the interval $\Delta t_1, \dots, \Delta t_4$ durations and take into account the accepted notation. As a result,

$$B_1(\Delta t_1) = B_3(\Delta t_3) = \begin{pmatrix} \frac{1 - \exp(-rD\beta)}{R} \\ 0 \end{pmatrix}; \quad (42)$$

$$B_2(\Delta t_2) = \begin{pmatrix} -\exp\left(-r\frac{1-D}{2}\beta\right) \frac{\sin\frac{1-D}{2}\beta}{\omega L} \\ 1 - \exp\left(-\frac{1-D}{2}\beta\right) \left(\cos\frac{1-D}{2}\beta + r \sin\frac{1-D}{2}\beta \right) \end{pmatrix}; \quad (43)$$

$$B_4(\Delta t_4) = \begin{pmatrix} \exp\left(-r\frac{1-D}{2}\beta\right) \frac{\sin\frac{1-D}{2}\beta}{\omega L} \\ 1 - \exp\left(-\frac{1-D}{2}\beta\right) \left(\cos\frac{1-D}{2}\beta + r \sin\frac{1-D}{2}\beta \right) \end{pmatrix}. \quad (44)$$

By making the operations in equation (12) and a series expansion, vector $B^{(1)}$ is found to be:

$$B^{(1)} = \begin{pmatrix} \frac{2rD}{R}\beta + \frac{r}{2} \cdot \frac{2r\omega L(D^2 - 3D) + R(1-D)}{R\omega L} \beta^2 + O(\beta^3) \\ \frac{r\omega L(1+r^2)D(1-D)}{2R} \beta^2 + O(\beta^3) \end{pmatrix}. \quad (45)$$

The steady-state values of the vector $X^{(1)}$ coordinates are found from equation (13) for k striving to infinity ∞ . Then, the partial transient will decay to zero, and it will be possible to equate the vectors at t_{k+1} and t_k . Denote the desired vector $X^{(1)(\infty)}$ –

$$X^{(1)(\infty)} = A^{(1)} X^{(1)(\infty)} + B^{(1)} \frac{V}{2}. \quad (46)$$

From equation (46), $X^{(1)(\infty)}$ becomes

$$X^{(1)(\infty)} = \begin{pmatrix} i_L^{(1)(\infty)} \\ v_C^{(1)(\infty)} \end{pmatrix} = (E - A^{(1)})^{-1} B^{(1)} \frac{V}{2}. \quad (47)$$

By calculating vector $X^{(1)(\infty)}$ components and making a power series expansion, $X^{(1)(\infty)}$ is eventually found to be:

$$X^{(1)(\infty)} = \begin{pmatrix} \frac{D}{R} - \frac{rD(1-D)}{2R} \beta - \frac{rD(1-D)(1-2D+D^2-r^2+2r^2D+r^2D^2)}{24R} \beta^2 + O(\beta^3) \\ 1 + \frac{\omega L(1+r^2)D(1-D)}{4R} \beta + O(\beta^2) \end{pmatrix} \frac{V}{2}. \quad (48)$$

Using vector $X^{(1)}$ coordinates for $k = \infty$, the particular solution of the non-homogeneous system can be represented as equation (30) with the replacement in Q_1 and Q_2 initial conditions $i_L(0)$ by $i_L(0) - i_L^{(1)(\infty)}$ and $v_C(0)$ by $v_C(0) - v_C^{(1)(\infty)}$ and addition of the term $X^{(1)(\infty)}$ on the right side.

An interesting specific case is making power-up for a "cold" converter, that is, a converter without energy stored in the reactive elements meaning zero initial conditions $i_L(0) = 0$ and $v_C(0) = 0$. Simple calculations lead to the following expressions –

$$i_L^{(1)}(k) = i_L^{(1)(\infty)} + I_1^{(1)} \lambda_1^k + I_2^{(1)} \lambda_2^k; \quad (49)$$

$$v_C^{(1)}(k) = v_C^{(1)(\infty)} + U_1^{(1)} \lambda_1^k + U_2^{(1)} \lambda_2^k; \quad (50)$$

$$I_1^{(1)} = \left(-\frac{D}{R} + \frac{(2\omega LrD - R)(1-D)}{4R\omega L} \beta + O(\beta^2) \right) \frac{V}{2}; \quad (51)$$

$$I_2^{(1)} = \left(\frac{1-D}{4\omega L} \beta + \frac{rD(1-D)}{8\omega L} \beta^2 + O(\beta^3) \right) \frac{V}{2}; \quad (52)$$

$$U_1^{(1)} = \left(-\frac{\omega L(1+r^2)D(1-D)}{4R} \beta + \frac{(2\omega LrD + RD - R)(1+r^2)(1-D)}{16R} \beta^2 + O(\beta^3) \right) \frac{V}{2}; \quad (53)$$

$$U_2^{(1)} = \left(-1 + O(\beta^2) \right) \frac{V}{2} \quad (54)$$

and $i_L^{(1)(\infty)}$, $v_C^{(1)(\infty)}$ from equation (48).

In the same way, it is possible to start the process with a topology corresponding to the time intervals Δt_2 , Δt_3 and Δt_4 . Each of these cases will have its own transition matrix that differs from matrix $A^{(1)}$ by a cyclic permutation of the factors. Partial transient processes for each case are different. However, the dynamic behaviour is the same because, as stated earlier, all these matrices have the same eigenvalues.

Figure 2 schematically illustrates the situation described. The greasy breaking line corresponds to a state-space vector coordinate (inductor current or capacitor voltage).

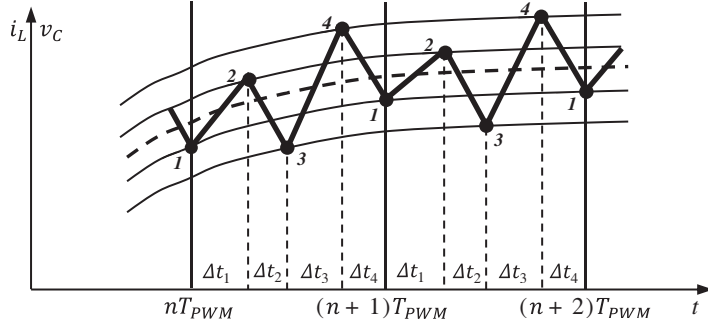


Fig. 2. Illustration of a behaviour of a generalised state-space variable in the converter

The points on the line correspond to the switching instants, that is, the moments of changing the FCC topology. The points numbering is done according to the number of the time interval from which the modulation period begins. The case analysed above is illustrated by a set of points with the number 1.

The cases where the process starts with the intervals Δt_2 , Δt_3 and Δt_4 correspond to the point sets 2, 3, and 4. The corresponding matrices, vectors, and coefficients for cases 2, 3, and 4 are distinguished by means of superscript indices with a number of set in parentheses. Then, the transition matrices and vectors of the right side are given by the following equations.

$$A^{(2)} = A_1(\Delta t_1)A_4(\Delta t_4)A_3(\Delta t_3)A_2(\Delta t_2); \quad (55)$$

$$B^{(2)} = A_1(\Delta t_1)\left(A_4(\Delta t_4)\left(A_3(\Delta t_3)B_2(\Delta t_2) + B_3(\Delta t_3)\right) + B_4(\Delta t_4)\right) + B_1(\Delta t_1). \quad (56)$$

$$A^{(3)} = A_2(\Delta t_2)A_1(\Delta t_1)A_4(\Delta t_4)A_3(\Delta t_3); \quad (57)$$

$$B^{(3)} = A_2(\Delta t_2)\left(A_1(\Delta t_1)\left(A_4(\Delta t_4)B_3(\Delta t_3) + B_4(\Delta t_4)\right) + B_1(\Delta t_1)\right) + B_2(\Delta t_2). \quad (58)$$

$$A^{(4)} = A_3(\Delta t_3)A_2(\Delta t_2)A_1(\Delta t_1)A_4(\Delta t_4); \quad (59)$$

$$B^{(4)} = A_3(\Delta t_3)\left(A_2(\Delta t_2)\left(A_1(\Delta t_1)B_4(\Delta t_4) + B_1(\Delta t_1)\right) + B_2(\Delta t_2)\right) + B_3(\Delta t_3). \quad (60)$$

The partial transient calculations for each of the three indicated cases are omitted as they follow those for the first case above and only the final results for $n = 2, 3$, and 4 are presented.

$$i_L^{(n)}(k) = i_L^{(n)}(\infty) + I_1^{(n)}\lambda_1^k + I_2^{(n)}\lambda_2^k; \quad (61)$$

$$v_C^{(n)}(k) = v_C^{(n)}(\infty) + U_1^{(n)}\lambda_1^k + U_2^{(n)}\lambda_2^k; \quad (62)$$

$$I_1^{(n)} = \left(-\frac{D}{R} + (-1)^{n-1} \frac{(2\omega LrD - R)(1-D)}{4R\omega L} \beta + O(\beta^2)\right) \frac{V}{2}; \quad (63)$$

$$I_2^{(n)} = \left(sw_1(n) \frac{1-D}{4\omega L} \beta + sw_2(n) \frac{rD(1-D)}{8\omega L} \beta^2 + O(\beta^3)\right) \frac{V}{2}; \quad (64)$$

$$U_1^{(n)} = \left(-sw_1(n) \frac{\omega L(1+r^2)D(1-D)}{4R} \beta + sw_2(n) \frac{(2\omega LrD + RD - R)(1+r^2)(1-D)}{16R} \beta^2 + O(\beta^3)\right) \frac{V}{2}; \quad (65)$$

$$U_2^{(n)} = (-1 + O(\beta^2)) \frac{V}{2}; \quad (66)$$

$$i_L^{(n)}(\infty) = \left(\frac{D}{R} + (-1)^n \frac{rD(1-D)}{2R} \beta - \frac{rD(1-D)(1-2D+D^2-r^2+2r^2D+r^2D^2)}{24R} \beta^2 + O(\beta^3) \right) \frac{V}{2}; \quad (67)$$

$$v_C^{(n)}(\infty) = \left(1 + sw_1(n) \frac{\omega L(1+r^2)D(1-D)}{4R} \beta + O(\beta^2) \right) \frac{V}{2}, \quad (68)$$

$$\text{where } sw_1(n) = \begin{cases} 1, & n=1, 2 \\ -1, & n=3, 4 \end{cases} \quad sw_2(n) = \begin{cases} 1, & n=1, 4 \\ -1, & n=2, 3 \end{cases}$$

The four partial transient processes are linear combinations of eigenfunctions defined at discrete points in time kT_{PWM} . In engineering practice, it is more convenient to use the functions defined on the entire time axis. The transition to such functions will be correct if they coincide with the original discrete ones at all points where they are defined and behave monotonously and smoothly in-between. In Figure 2, graphs of such functions are schematically represented by the thin lines passing through equally numbered points.

To proceed to the continuous model, the discrete functions λ_i^k should be continued on the entire time axis and replaced with exponential terms $\exp(\sigma_i t)$, so that $\lambda_i^k = \exp(\sigma_i k T_{\text{PWM}})$. It follows that $\sigma_i = \ln(\lambda_i) / T_{\text{PWM}}$. Substitution of equations (25) for λ_1 and (26) for λ_2 followed by a power series expansion yields the following expressions:

$$\sigma_1 = \frac{1}{T_{\text{PWM}}} \left(-2r\beta + \frac{r(1+r^2)(2D+1)(1-D)^2}{24} \beta^3 + O(\beta^4) \right); \quad (69)$$

$$\sigma_2 = \frac{1}{T_{\text{PWM}}} \left(-\frac{r(1+r^2)(2D+1)(1-D)^2}{24} \beta^3 + O(\beta^4) \right). \quad (70)$$

6. Natural balancing dynamics

Let us define the FCC transient as the arithmetic average of the four partial transients (dashed curve in Figure 2). Such a definition seems to be quite natural since in this case the actual process (thick broken line in Figure 2) can be represented as the sum of a slow transition process and high-frequency oscillations superimposed on. The average value of such oscillations is zero, and they can be filtered by a low-pass filter.

According to this definition, the transient expressions for the inductor current and capacitor voltage can be written as:

$$i_L^{(av)}(t) = i_L^{(av)}(\infty) + I_1^{(av)} \exp(\sigma_1 t) + I_2^{(av)} \exp(\sigma_2 t); \quad (71)$$

$$v_C^{(av)}(t) = v_C^{(av)}(\infty) + U_1^{(av)} \exp(\sigma_1 t) + U_2^{(av)} \exp(\sigma_2 t), \quad (72)$$

where

$$i_L^{(av)}(\infty) = \left(\frac{D}{R} - \frac{(1-D)(r^2(1+D)^2 + (1-D)^2)}{24R} \beta^2 + O(\beta^3) \right) \frac{V}{2},$$

$$I_1^{(av)} = \left(-\frac{D}{R} + O(\beta^2) \right) \frac{V}{2}, I_2^{(av)} = O(\beta^3) \frac{V}{2}, v_C^{(av)}(\infty) = \left(1 + O(\beta^2) \right) \frac{V}{2},$$

$$U_1^{(av)} = \left(-\frac{(1+r^2)(1-D)^2}{16} \beta^2 + O(\beta^3) \right) \frac{V}{2}, U_2^{(av)} = \left(-1 + O(\beta^2) \right) \frac{V}{2}.$$

Neglecting higher order terms for $i_L^{(av)}(\infty)$, $I_1^{(av)}$, $v_C^{(av)}(\infty)$, $U_1^{(av)}$, and $U_2^{(av)}$, and also neglecting $I_2^{(av)}$ compared with $I_1^{(av)}$ and $U_1^{(av)}$ compared with $U_2^{(av)}$ yields

$$i_L^{(av)}(t) = V \frac{D}{2R} \left(1 - \exp(\sigma_1 t) \right); \quad (73)$$

$$v_C^{(av)}(t) = \frac{V}{2} \left(1 - \exp(\sigma_2 t) \right). \quad (74)$$

After performing the same procedure over the exponent indicators (equations (69) and (70)), their expressions are simplified to $\sigma_1 = -\frac{2r}{T_{\text{PWM}}} \beta$, $\sigma_2 = -\frac{r(1+r^2)(2D+1)(1-D)^2}{24T_{\text{PWM}}} \beta^3$. Substituting instead of r and β their expressions, after elementary transformations the exponent indicator expressions are obtained as $\sigma_1 = -\frac{R}{L}$ and $\sigma_2 = -\frac{RT_{\text{PWM}}^2}{48L^2C} (2D+1)(1-D)^2$ that corresponds to the time constants obtained in the study by Margaliot et al. (2011) (equations (28) and (32)).

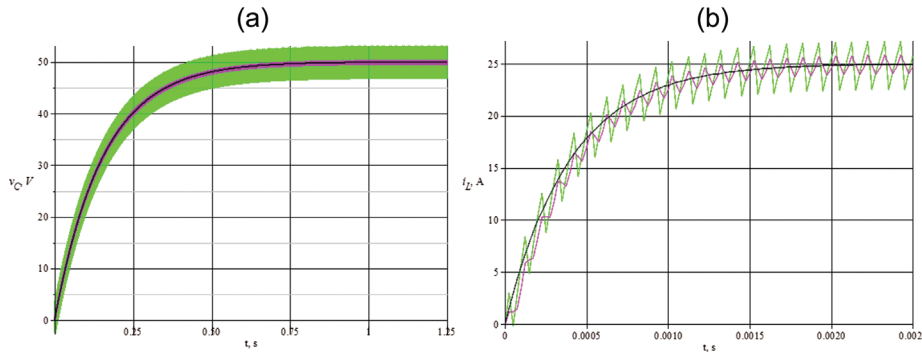


Fig. 3. Capacitor voltage (a) and inductor current (b) transient in the converter

7. Discussion

In Figure 3, the numeric simulation results are compared with theoretical calculations for the following parameters: $L = 0.0004 \text{ H}$, $C = 0.0001 \text{ F}$, $R = 1 \text{ Ohm}$, $T_{\text{PWM}} = 0.0001 \text{ s}$, $D = 0.5$, $V = 100 \text{ V}$.

Figure 3a shows the graphs of the capacitor voltage simulation (the green curve) and the transition process calculated by equation (74) (the black curve). Figure 3b shows similar curves for the inductor current. Black curve is calculated by equation (73). Magenta curves on both pictures correspond to simulation curves filtered by a first-order filter with a time constant T_f . For the voltage curve, the time constant was selected $T_f = T_{\text{PWM}}$, for the current curve $T_f = T_{\text{PWM}}/4$. Both figures show good agreement between the simulation and calculation results.

Despite the fact that the transients for inductor current and capacitor voltage are described by linear combinations of two exponential terms, in practice they differ very little from purely exponential curves (fast for inductor current and slow for capacitor voltage) because the contribution of the second exponential term is practically negligible.

The voltage exponent decays much slowly compared with the current one because for the selected parameters $\sigma_1 = -2500\text{s}^{-1}$, $\sigma_2 = -6.51\text{s}^{-1}$. The current steady-state value amounts to $i_L^{(av)}(\infty) = V \frac{D}{2R} = 25\text{A}$, the same for voltage $v_C^{(av)}(t) = \frac{V}{2} = 50\text{V}$.

8. Conclusion

The article presents the time domain analysis of three-level DC–DC FCC. The obtained analytical equations (73) and (74) are very simple and at the same time accurately describe the “long” time processes in the converter. The theoretical curves on the graphs practically coincide with the accurate simulation ones with the oscillations averaged by the low pass filter.

References

- Margaliot, M., Ruderman, A. and Reznikov, B. (2011). Mathematical Analysis of A Flying Capacitor Converter: A Sampled-Data Modeling Approach. *International Journal of Circuit Theory and Applications*, 41(7), pp. 82–700.
- McGrath, B. P. and Holmes, D. G. (2008). Analytical Modelling of Voltage Balance Dynamics for a Flying-Capacitor Multilevel Converter. *IEEE Transactions on Power Electronics*, 23(2), pp. 543–550.
- Meynard, T. A., Fadel, M. and Aouda, N. (1997). Modeling of Multilevel Converters. *IEEE Transactions on Industrial Electronics*, 44(3), pp. 356–364.
- Meynard, T. A. and Foch, H. (1992). Multilevel choppers for high voltage applications. *European Power Electronics and Drives Journal*, 2, pp. 45–50.
- Ruderman, A. and Reznikov, B. (2011). Seven-level single-leg flying capacitor converter voltage balancing dynamics analysis. In: *Proceedings of 14th European Conference on Power Electronics and Applications*, Birmingham (Great Britain), October 2011, pp. 1–10.
- Ruderman, A., Reznikov, B. and Margaliot, M. (2008). Simple analysis of a flying-capacitor converter voltage balance dynamics for DC modulation. In: *Proceedings of 13th International Power Electronics and Motion Control Conference*, Poznan (Poland), September 2008, pp. 260–267.
- Wilkinson, R. H., Meynard, T. A. and du Toit Mouton, H. (2006). Natural Balance of Multicell Converters: The General Case. *IEEE Transactions on Power Electronics*, 21(6), pp. 1658–1666.

